

Effect of Inclusion Size on Fatigue Properties in Very High Cycle Region of Low Alloy Steel Used for Solid type Crankshaft

Ryota YAKURA*¹, Mariko MATSUDA*¹, Dr. Tatsuo SAKAI*², Dr. Akira UENO*²

*¹ Technical Development Dept., Steel Casting & Forging Div., Iron & Steel Business

*² Dept. of Mechanical Engineering, College of Science and Engineering, RITSUMEIKAN Univ.

A study was conducted to grasp the fatigue properties, including the properties in a very high cycle fatigue region, of a low-alloy steel used for the solid type crankshaft of a 4-cycle diesel engine. Fatigue tests were conducted on specimens, some of which were taken from a solid type crankshaft and others taken from a round forged bar. The relation between the inclusion size at crack initiation sites and the fatigue property was studied on the basis of fracture mechanics. The study developed a relation equation between the fatigue life and inclusion size, as well as a relation equation between the threshold stress intensity range and inclusion size, for fracture initiated from the surface and internal inclusions. These equations show that decreasing inclusion size improves not only the fatigue strength working against surface fracture but also that attributable to internal fracture.

Introduction

Higher output and smaller size are desired for 4 cycle diesel engines for marine and onshore power generators.¹⁾⁻⁴⁾ This requires greater strength in solid type crankshafts for 4-cycle diesel engines. Therefore, low alloy steel having a tensile strength of 900-1,100MPa is being mainly used as the material.

Kobe Steel is focusing on the development of technologies for increasing fatigue strength, in addition to the strength of the material. Large steel forgings such as solid type crankshafts inevitably contain inclusions. These inclusions are known to become the initiation sites of fatigue cracks and decrease the fatigue strength in accordance with their sizes.⁵⁾ The company has therefore decreased the amount and size of the inclusions contained in steel forgings and thus developed super clean steels with improved fatigue strength.⁶⁾⁻⁸⁾ These steels are being applied to solid type crankshafts.

A solid type crankshaft is subjected to as many as 10^9 cycles of stress during the entire service life of a 4-cycle diesel engine. The fatigue up to 10^9 cycles of stress is called very high cycle fatigue, which is the focus of many studies.⁹⁾ Although the materials of solid type crankshafts require understanding of their fatigue characteristics up to a very high cycle region, there are only a few examples of such studies.^{10), 11)} Against this backdrop, fatigue tests were performed

on low alloy steels for solid type crankshafts to confirm the presence of fatigue fractures in the very high cycle region and the effect of inclusion size on fatigue limits. A study was conducted on the relationship of fatigue life and fatigue limit to inclusion size.

1. Features of fatigue fractures in very high cycle region

Conventional thought has been that the fatigue fracture of steel does not occur unless the stress exceeds the fatigue limit appearing at 10^7 stress cycles (hereinafter simply referred to as "fatigue limit") More recent studies, however, have clarified the existence of phenomena in which fatigue fractures occur at 10^7 to 10^9 cycles under stress lower than the fatigue limit, particularly in the case of high strength steel; this phenomenon is referred to as very high cycle fatigue.

The usual fatigue fractures are initiated from metal surfaces or from inclusions existing in surface layers (hereinafter referred to as "surface inclusions"); meanwhile, in the case of very high cycle fatigue fractures, the initiation sites of cracks are generally believed to be inclusions below surface layers (hereinafter referred to as "internal inclusions.")⁹⁾ Such very high cycle fatigue fractures, initiated from internal inclusions, are considered to occur more often in bearing steel,¹²⁾ spring steel¹³⁾ and tool steel,¹⁴⁾ for example, or in high strength steel having a tensile strength of 1,200MPa or greater.¹⁵⁾ It is not clear, however, if very high cycle fatigue fractures occur in the low alloy steels for solid type crankshafts, which exhibit a tensile strength of approximately 900-1,100MPa.

2. Research and test method

2.1 Test materials

Test materials were made from steel ingots weighing 12 to 65 tonnes. The test steels included 40CrMo8, developed by Kobe Steel, as well as 34CrNiMo6, 36CrNiMo4 and 42CrMo4 (DIN standard steel). **Table 1** shows the target compositions of these steels and the amount ranges

Table 1 Target chemical composition of test steels

Material	(mass%)							S	O
	C	Si	Mn	Ni	Cr	Mo			
40CrMo8	0.38	0.25	0.90	-	2.00	0.25			
34CrNiMo6	0.34	0.25	0.65	1.50	1.50	0.25	<60	<50	
36CrNiMo4	0.36	0.25	0.65	1.00	1.00	0.25	ppm	ppm	
42CrMo4	0.42	0.25	0.75	-	1.10	0.23			

of S and O. In the case of 40CrMo8, adjustment was made on the amounts of S and O, as well as on slag compositions, etc., to control the size of inclusions, and both super clean steel (S<20 ppm, O<15 ppm) and conventional grade steel were prepared.

These steel ingots were hot-forged at a forging ratio of 3.0 or greater to form round bars with diameters of ϕ 450-620mm. In addition, two steel ingots of 40CrMo8, one consisting of super clean steel and the other consisting of conventional grade steel, each weighing approximately 65 tonnes, were hot-forged into solid type crankshafts with a principal axis diameter of 480mm.

The formed materials were subjected to quenching and tempering. The round bars were tempered to the tensile strength range of 800 to 1,100MPa, while the crankshafts were tempered to a tensile strength class of 1,000MPa (in the range of 950 to 1,050MPa).

Test specimens were prepared as shown in Fig. 1. In the case of the crankshafts, specimens were collected from their pin fillet, where the greatest load would be applied during operation; and, in the case of the round bars, each specimen was taken such that it was equivalent with the specimens from crankshaft pin fillets in terms of the depth from the surface and the direction of grain flow against the longitudinal direction of the specimen.

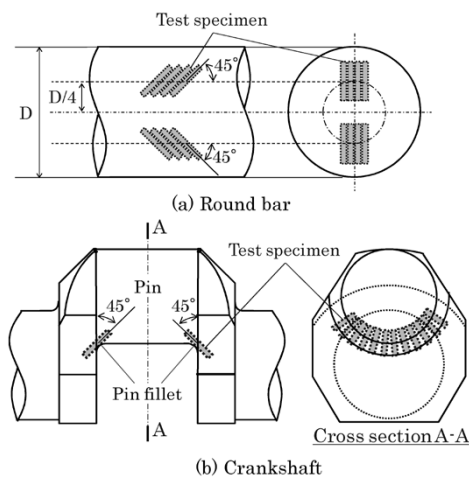


Fig. 1 Preparation of specimens

2.2 Fatigue test

2.2.1 High cycle fatigue test

Rotating bending fatigue tests were performed on the super clean steel and conventional grade steel to compare their fatigue limits up to 10^7 cycles. In addition, the specimens collected from the crankshafts were subjected to axial load fatigue tests.

The rotating bending fatigue tests were conducted at a frequency of 60Hz on smooth specimens, each taken from the round bar and having a parallel portion of ϕ 10 x 30mm. A difference method was applied for the tests to determine the fatigue limit σ_w for each specimen. More specifically, each fatigue test was conducted at stress amplitude σ_a , and if no failure occurred at 3×10^6 cycles, the σ_a was increased by increments of 20MPa, continuing the test until failure occurred. The failure stress (σ_a) minus 20MPa was determined to be σ_w . This method enables a directly study of the relationship between σ_w and the inclusion size.

An axial load fatigue test was performed using a smooth specimen having a parallel portion of ϕ 10 x 30mm, at a stress ratio of -1. The tests were conducted at frequencies of 30 to 45Hz and were aborted at 10^7 cycles.

2.2.2 Very high cycle fatigue test

In order to compare the fatigue characteristics up to the very high cycle region of super clean steel and conventional grade steel, cantilever rotating bending fatigue tests¹⁶⁾ were performed. Each specimen was taken from the crankshaft material, as in the case of the axial load fatigue test specimens, and had a sandglass shape with a minimum cross-sectional diameter of ϕ 4mm. The tests were conducted at a frequency of 52.5Hz and were aborted at 10^9 cycles. It should be noted that all the above fatigue tests were performed in air at ambient temperature.

2.3 Observation of fracture surface and measurement of inclusion size

The fracture surfaces of failed specimens were observed by SEM. When the initiation site of a fatigue crack was an inclusion, the shape of the inclusion was approximated by a circumscribing ellipse, and the square root of the ellipse area, \sqrt{area} , was regarded as the value representing the inclusion size. The value of \sqrt{area} is known to be an effective parameter for evaluating the effect of inclusion size on fatigue strength.⁵⁾

3. Test results

3.1 Results of high cycle fatigue tests

Fig. 2 shows the fatigue limits (σ_w) obtained by the rotating bending fatigue test, for the 40CrMo8 super clean steel compared with the conventional grade steel, including 40CrMo8 and other three grades, all in the 800-1,100MPa strength range. Although dispersion was observed in the data of both the super clean steel and conventional grade steel, increasing the tensile strength tended to increase fatigue limits. It was found that, although the upper limits of the dispersion were similar for the super clean steel and conventional grade steel, the lower limit was higher for the super clean steel. In other words, the σ_w of the super clean steel is said to be consistently higher than that of the conventional grade steel.

Fig. 3 shows the results of axial load fatigue tests on the super clean steel and conventional grade steel of 40CrMo8. The axial load fatigue tests were performed, focusing on the stress amplitudes that are considered, from the results of the rotating bending fatigue tests, to be in the vicinity of the fatigue limits. The axial load fatigue tests have confirmed two fracture modes; in one, the fatigue cracks are initiated from surface inclusions

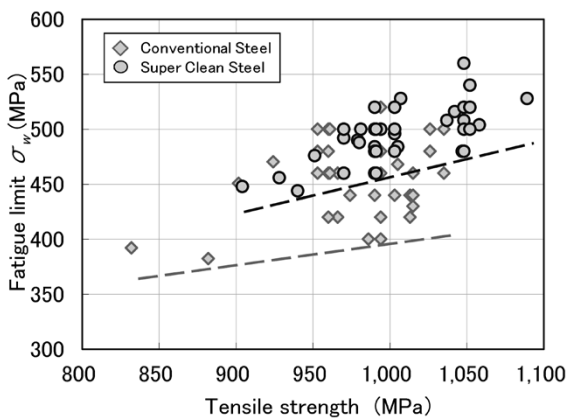


Fig. 2 Results of rotating bending fatigue tests

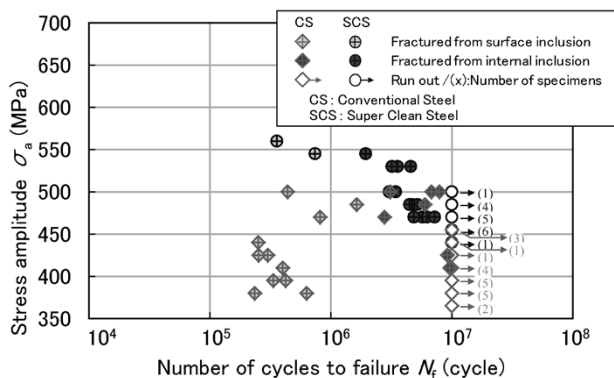


Fig. 3 Results of axial load fatigue tests on 40CrMo8

and, in the other, they are initiated from internal inclusions. The fatigue fractures initiated from surface inclusions mainly occurred at under 10^6 cycles, whereas all the fatigue fractures initiated from internal inclusions occurred at 10^6 cycles or higher. Referring to the minimum stress amplitudes at which failures occurred, the amplitudes were 545MPa and 380MPa for the super clean steel and conventional grade steel, respectively, in the case of fractures initiated from surface inclusion, and were 545MPa and 380MPa for the super clean steel and conventional grade steel, respectively, in the case of fractures initiated from internal inclusions. In either case, the super clean steel exhibited a higher stress amplitude.

3.2 Results of very high cycle fatigue tests

The super clean steel and conventional grade steel of 40CrMo8 were subjected to cantilever rotating bending fatigue tests and the results are shown in Fig. 4. The super clean steel and conventional grade steel exhibited a σ_w of 582.5MPa and 525MPa, respectively, the former being approximately 11% higher than the latter. All the fatigue cracks initiated from the metal surface in the case of the super clean steel, but from the surface inclusions in the case of the conventional grade steel. There was no fracture initiated from an internal inclusion, as seen in the axial load fatigue test, and the same can be said of fatigue fractures in the 10^6 - 10^9 cycle range.

3.3 Results of fracture surface observation

Fig. 5 shows the examples of fracture surfaces in backscattered electron images captured by SEM. As described above, three types of fatigue-crack initiation sites were observed: namely, metal surfaces (Fig. 5 (a)), surface inclusions (Fig. 5 (b)) and

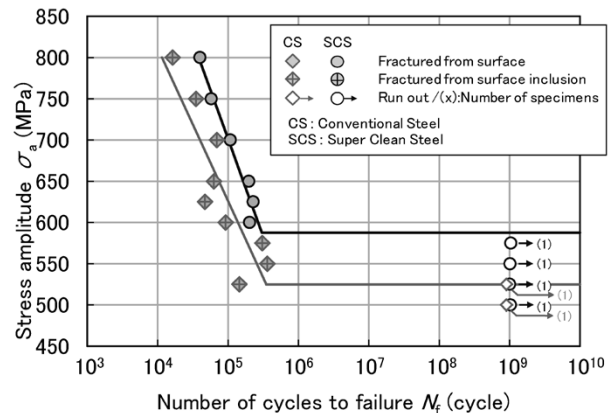


Fig. 4 Results of cantilever rotating bending fatigue test on 40CrMo8

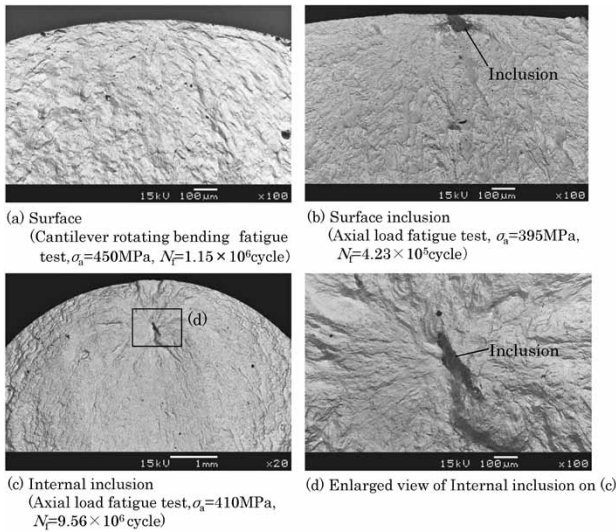


Fig. 5 Examples of fatigue crack initiation sites

internal inclusions (Fig. 5 (d), which is an enlarged view of (c) with focus on the inclusion in (c)). The sizes of the inclusions (\sqrt{area}) were approximately 20 to 60 μm for the super clean steel and 20 to 150 μm for the conventional grade steel.

4. Discussions

4.1 S-N relationship corresponding to fracture modes

Fig. 6 shows the collective results of the cantilever rotating bending fatigue tests and axial load fatigue tests. In Fig. 6, the super clean steel and conventional grade steel are not distinguished, and different data points are used depending on the test methods and fracture modes. It appears from Fig. 6 that an S-N relationship holds for each of the fatigue crack initiation sites, namely, metal surfaces (Surface), surface inclusions (Surface inclusion) and internal inclusions (Internal inclusion). The fatigue life was shortest for fatigue cracks initiated from surface inclusions, shorter for those initiated from metal surfaces, and longest for those initiated from internal inclusions. The fractures initiated from surface inclusions exhibited a lower minimum failure stress than did the fractures initiated from internal inclusions. The possibility cannot be denied, however, that fracture initiated from an internal inclusion may occur in the cycle range beyond 10^7 at a stress amplitude lower than the minimum failure stress determined for the fractures initiated from surface inclusions, since the axial load fatigue tests were aborted at 10^7 cycles. In the case of the cantilever rotating bending fatigue tests, no fatigue fracture was due to an internal inclusion in the long-life range (10^{6-9} cycles); however, the specimen size,

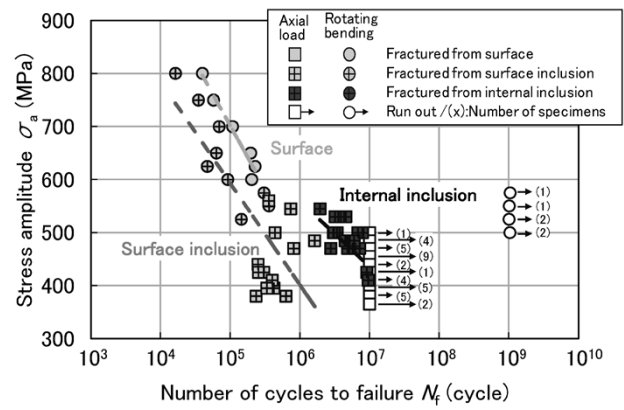


Fig. 6 Results of axial load and cantilever rotating bending fatigue tests on 40CrMo8

which is smaller than the one for the axial load fatigue tests, may have resulted in a smaller number of internal inclusions, which may have led to the non-appearance of any fracture initiated from an internal inclusion. In other words, it was not yet clear, at this point, whether any fracture initiated from an internal inclusion occurs in the range beyond 10^7 cycles and what the S-N relationship would be. Against this backdrop, the following study was conducted to predict the behavior of fractures initiated from internal inclusions in the range beyond 10^7 cycles.

4.2 Relationship between fatigue life and inclusion size

The initial stress intensity factor range, ΔK , assuming the inclusion to be a crack, is expressed by Equation (1) based on \sqrt{area} and stress amplitude, σ_a .⁵⁾

$$\Delta K = M \sigma_a (\pi \sqrt{area})^{1/2} \dots \dots \dots (1)$$

wherein M is the correction coefficient for the stress intensity factor and is known to be 0.65 for fatigue cracks initiated from surface inclusions and 0.50 for those initiated from internal inclusions.⁵⁾ Also, it is believed that a double logarithmic linear relationship, as expressed by Equation (2), holds between the ΔK determined by Equation (1) and a parameter, N_f / \sqrt{area} , determined by dividing fatigue life N_f by \sqrt{area} .¹⁰⁾

$$\Delta K = a (N_f / \sqrt{area})^\beta \dots \dots \dots (2)$$

On the basis of the results of the axial-load and cantilever rotating bending fatigue tests on 1,000MPa class 40CrMo8, as well as the results of the fracture surface observation by SEM, the relationships between ΔK and (N_f / \sqrt{area}) were plotted; the results are shown in Fig. 7. It was estimated from Fig. 7 that the a in Equation (2) is 25 for fractures initiated from surface inclusions and 44 for fractures initiated from internal inclusions, while β is -0.21

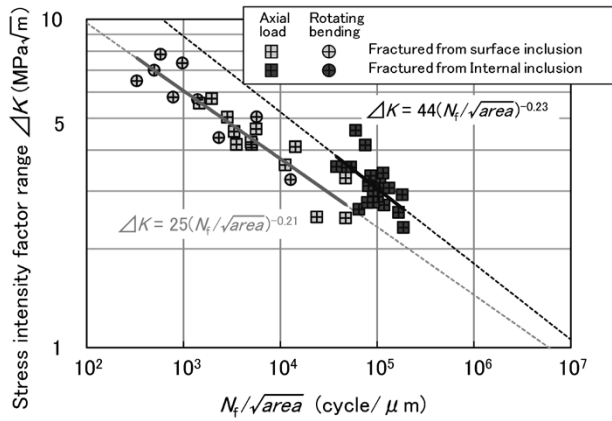


Fig. 7 Relationship between ΔK and (N_f/\sqrt{area}) for 40CrMo8

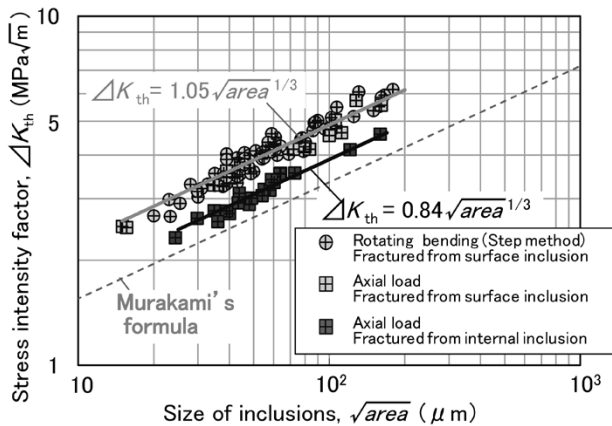


Fig. 8 Relationship between ΔK_{th} and \sqrt{area} for 40CrMo8

for fractures initiated from surface inclusions and -0.23 for fractures initiated from internal inclusions. On the basis of Equation (2), as well as α and β determined from Fig. 7, N_f for surface and internally-initiated fractures can be estimated for any given σ_a and \sqrt{area} .

4.3 Relationship between fatigue limit and inclusion size

In general, the fatigue limit of steel is believed to correspond, not to the generation limit of cracks, but rather, to the arrest limit of crack propagation.⁵⁾ Therefore, clarifying the relationship between the lower limit of the stress intensity factor range, ΔK_{th} , the threshold for cracks to start propagation, and \sqrt{area} clarifies the effect of inclusion size on fatigue limit.

Fig. 8 shows the results of the rotating bending fatigue test and axial load fatigue test on 1,000MPa class 40CrMo8, as well as the plots of ΔK , calculated by Equation (1) on the basis of the SEM fracture surface observation, against the experimental values of \sqrt{area} .

The rotating bending fatigue tests, based on

a difference method, provide σ_w and for each specimen. These values are assigned to σ_a and \sqrt{area} of Equation (1), which provide ΔK that can be regarded as the threshold, ΔK_{th} , at which fatigue cracks start to propagate.

Meanwhile, ΔK calculated by assigning the failure stress, σ_b , obtained by the axial load fatigue tests, and \sqrt{area} value into σ_a and \sqrt{area} of Equation (1) cannot be regarded as ΔK_{th} per se. In this study, however, the above described ΔK is treated as ΔK_{th} to formulate the relationship between ΔK_{th} and \sqrt{area} for fractures initiated from internal inclusions, due to the facts that the axial load fatigue tests were performed under the stress amplitudes considered to be in the vicinity of the fatigue limit, and that the data points for the fractures initiated from surface inclusions of the difference method and axial load fatigue test were in agreement.

Because a tendency similar to Murakami's equation,⁵⁾ expressed by Equation (3), was recognized for both the fractures initiated from the surface and those initiated from internal inclusions in Fig. 8, ΔK_{th} was assumed to be proportional to $\sqrt{area}^{1/3}$ to provide Equation (4).

$$\Delta K_{th} = 3.3 \times 10^{-2} (HV+120 (\sqrt{area})^{1/3}) \dots\dots\dots (3)$$

$$\Delta K_{th} = \gamma (\sqrt{area})^{1/3} \dots\dots\dots (4)$$

From Fig. 8, the coefficient γ for fractures initiated from surface inclusions was estimated to be 1.05, while the one for fractures initiated from internal inclusions was estimated to be 0.84 in the case of 1,000MPa class 40CrMo8. Furthermore, from Equation (4), ΔK_{th} for fractures initiated from internal inclusions can be estimated for any given \sqrt{area} , and it is thus possible to calculate σ_w , as will be described in the next section.

4.4 Estimation of S-N curve and estimation on the effect of inclusion size

On the basis of Equations (1) and (2), which relate ΔK to N_f and \sqrt{area} , along with Equation (4), expressing the relationship between ΔK_{th} and \sqrt{area} , S-N curves can be calculated for fractures initiated from both surface and internal inclusions having any given size.

Firstly, the inclusion size is assumed to be \sqrt{area} , and a stress amplitude $\sigma_{a,i}$ is assigned to Equation (1) to calculate the stress intensity factor range, ΔK_i , corresponding to $\sigma_{a,i}$. Assigning the calculated ΔK_i and \sqrt{area} to Equation (2) determines the number of cycles to failure, $N_{f,i}$ corresponding to \sqrt{area} and $\sigma_{a,i}$. Determining $N_{f,i}$ for other $\sigma_{a,i}$ values in a similar manner enables the calculation of an S-N curve within a finite life region, as shown by the curve ① in Fig. 9. Next, using Equation (1) to determine the

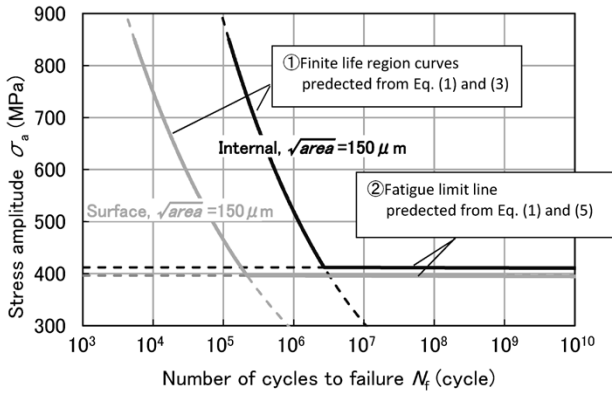


Fig. 9 Method of calculating S-N curves

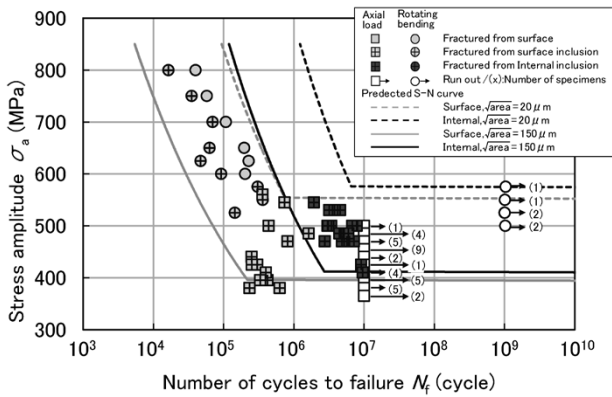


Fig.10 S-N curves calculated for 40CrMo8

stress amplitude corresponding to the threshold stress intensity range ΔK_{th} , which is given by assigning \sqrt{areae} to Equation (4), σ_w and the straight line ② are obtained. As shown in Fig. 9, eliminating the portion of the curve ① below the intersection between curve ① and straight line ②, along with the left side portion of the straight line ②, provides an S-N curve.

Fig.10 shows estimated S-N curves. Since the sizes of inclusions observed on the fracture surface of the fatigue specimens fell in the range of $\sqrt{areae} = 20\text{-}150\ \mu\text{m}$, the S-N curves for fractures initiated from the surface and internal inclusions were calculated under the two conditions of the lower limit, $20\ \mu\text{m}$, and the upper limit, $150\ \mu\text{m}$.

The results show that almost all data points for the fractures initiated from the surface and internal inclusions fall between the S-N curves calculated for $\sqrt{areae} = 20\ \mu\text{m}$ and $\sqrt{areae} = 150\ \mu\text{m}$ of respective fracture mode. Furthermore, the maximum value of σ_a ($=575\text{MPa}$), at which no failure occurred at 10^9 cycles of the cantilever rotating bending fatigue test, roughly matched σ_w (the horizontal portion) of the S-N curve calculated for the fracture initiated from an internal inclusion of $\sqrt{areae} = 20\ \mu\text{m}$. From the above results, the S-N curves calculated by the present technique are believed to be reasonable.

On the basis of the calculated S-N curves in

Fig.10, the following can be said for the fatigue characteristics, including the very high cycle region, of $1,000\text{MPa}$ class 40CrMo8. First, the comparison of the S-N curves calculated for $\sqrt{areae} = 20\ \mu\text{m}$ and $150\ \mu\text{m}$ shows that the position of the S-N curves for $\sqrt{areae} = 20\ \mu\text{m}$ is position on the long-life side of the figure with a higher σ_w , than the one for $\sqrt{areae} = 150\ \mu\text{m}$ in the case of fractures initiated from a surface as well as those initiated from internal inclusion. This result indicates that super clean steel, having reduced inclusion size, can have improved fatigue limits, not only for the fractures initiated from surface inclusions, but also for the fractures initiated from internal inclusions. In addition, the comparison between the S-N curves calculated for the fracture initiated from an internal inclusion and fracture initiated from a surface inclusion, both the inclusions having the same \sqrt{areae} , shows that a fracture initiated from an internal inclusion indicates a σ_w higher than that of a fracture initiated from a surface inclusion. In other words, in the case where inclusions of the same size exist in the surface layer and interior, no fatigue fracture occurs from the internal inclusion under a stress equal to or below σ_w for the fracture initiated from a surface inclusion. Furthermore, each S-N curve has a sloped portion and horizontal portion intersecting at a position lower than 10^7 cycles. This implies that, in the high cycle region at or beyond 10^7 cycles, neither fracture initiated from the surface nor fracture initiated from internal inclusion will occur.

Conclusions

Fatigue characteristics including the very high cycle region were studied for super clean steel and the conventional grade steel used for solid type crankshafts. The effect of inclusion size on the fatigue life and fatigue limit was also studied. The following describes the results obtained:

- 1) Cantilever rotating bending fatigue tests, up to the maximum of 10^9 cycles, showed no fatigue fracture at or beyond 10^7 cycles for both the super clean steel and conventional grade steel.
- 2) A relational expression was obtained for the relationship between the fatigue life, N_f , and inclusion size, \sqrt{areae} , for fractures initiated from surfaces and internal inclusions of a low alloy steel manufactured by Kobe Steel for solid type crankshafts. A relational expression was also obtained for the threshold stress intensity range, ΔK_{th} , and inclusion size, \sqrt{areae} .
- 3) The relational expressions in 2) enable the calculations of S-N curves for both the fractures initiated from the surface and from an internal

inclusion for the inclusion size range of $\sqrt{\text{area}}$
= 20-150 μm .

- 4) It is considered that reducing the inclusion size can improve not only the fatigue limit due to fractures initiated from surface inclusions, but also the fatigue limit due to fractures initiated from internal inclusions.

References

- 1) M. Makabe. *Proceedings of 75th Conference on Marine Engineering*. 2006, p.77.
- 2) F. Koch. *The new MAN B&W L21/31 Engine-Design Development and Experience*. 2004, No.174.
- 3) J. Kytola. *Development of the Waertsilae 4-stroke engine*. 2004, No.123.
- 4) Y. Miyawaki et al. *The new DAIHATSU DC-17 4-stroke medium speed diesel engine*. 2004, No.101.
- 5) Y. Murakami. *Metal Fatigue: Effects of Small Defects and Nonmetallic Inclusions*. 1993.
- 6) T. Shinozaki et al. *R&D Kobe Steel Engineering Reports*. 2009, Vol.59, No.1, pp.94-97.
- 7) T. Shinozaki, et al. *International Symposium on Marine Engineering*. 2009.
- 8) R. Yakura, et al. *CIMAC Congress (2013)*. Paper No.442.
- 9) Tatsuo Sakai. *Journal of Solid Mechanics and Materials Engineering*. 2009, Vol.3, No. 3, pp.425-439.
- 10) S. Omata et al. *Journal of the Japan Institute of Marine Engineering*. 2003, Vol. 38, No.7, pp.55-62.
- 11) R. Yakura et al. *Proceedings of the 63rd JSMS Annual Meetings*. 2014, Presentation Number 206.
- 12) T. Sakai et al. *Journal of Society of Material Science Japan*. 2000, Vol.49, No.7, pp.779-785.
- 13) T. Abe et al. *Transactions of the Japan Society of Mechanical Engineers (A)*. 2001, Vol.67, No.664, pp.112-119.
- 14) K. Shiozawa et al. *Proceedings of the annual meeting of JSME/MMD*. 2001, pp.243-244.
- 15) K. Kanazawa et al. *NRIM Fatigue Data Sheet Technical Document*. 1989, No.9.
- 16) T. Yamamoto et al. *Proceedings of VHCF-5*. 2011, pp.439-444.